Essential Readings in Light Metals: Cast Shop for Aluminum Production.
Edited by John F. Grandfield and Dmitry G. Eskin.

Light Metals — From *Light Metals 2000*, Ray D. Peterson, Editor

HETEROGENEOUS NUCLEATION OF α-Al IN Al-Ni-Si ALLOYS

B.J. McKay, P. Cizek, P. Schumacher, & K.A.Q. O'Reilly.
Oxford Centre for Advanced Materials and Composites, Oxford University, Parks Road, Oxford, OX1 3PH, United Kingdom.

Abstract

In order to elucidate the detrimental effect of high Si contents on the grain refinement of Al alloys, the heterogeneous nucleation of α-Al in an $Al_{70}Ni_{13}Si_{17}$ (at.%) alloy was studied using a novel metallic glass technique. A Ti-B-Al 5:1 grain refiner rod containing TiB_2 particles, on which Al_3Ti layers were detected, was added to an $Al_{70}Ni_{13}Si_{17}$ melt that was subsequently rapidly quenched to form a metallic glass. The nucleation events, which occurred during quenching, were examined using transmission electron microscopy and energy-dispersive X-ray spectroscopy. No α-Al nucleation was detected on added boride particles although nucleation of an unidentified phase occasionally occurred on their non-basal faces. Nevertheless, α-Al was systematically observed to nucleate on hexagonal dendrites present in the melt, which implies that Si poisoning of the boride particles is occurring. The increased Si content appeared to be responsible for the weakening of the Al_3Ti layer, originally present on the surface of the boride particles in the grain refiner rod, which resulted in a reduction in the ability of these particles to nucleate α-Al.

Introduction

Silicon is an important addition to Al in casting technological processes. It increases the fluidity of the melt, thereby enabling an increase in the casting speed and facilitates the reliable casting of complex shapes. As a result, the addition of Si can substantially reduce costs. It is also common practice for Ti-B-Al grain refiner rods to be added to the melt. These contain potent TiB_2 particles that provide sites for the heterogeneous nucleation of α-Al, thus ensuring microstructural refinement. The resulting small equiaxed grain size reduces porosity, hot tearing, and cracking, whilst improving the mechanical properties and the uniformity of the microstructure. The uniformity of grain size, and thus its control in cast house practice, is becoming particularly important, as industry continuously demands products of a higher specification. However, research [1,2,3] has indicated that Si reduces the efficacy of grain refiner particles in microstructural refinement above addition levels of approximately 3 wt. %. This phenomenon is generally referred to as "silicon poisoning" [1].

In order to further improve the control of the as-cast microstructure, a greater understanding of the solidification process is required. This process is a combination of both nucleation and growth mechanisms. Growth can be easily examined using conventional grain refiner studies. However, in these methods, observation of nucleation events is obscured by subsequent growth. Recently, a novel metallic glass technique has been implemented [4,5,6] that allows direct observation of these events. In this technique, grain refiner particles are added to the melt, which is rapidly quenched to form a metallic glass matrix. During this process, the growth of α-Al nuclei formed heterogeneously on the refiner particles is halted at an early stage at the glass transition temperature, T_g. These nuclei embedded in

the metallic glass may be readily studied using transmission electron microscopy (TEM). As the nucleation occurs in an undercooled melt, the process is analogous to conventional solidification.

Previous research [4], using the metallic glass technique in an Al-Y-Ni-Co alloy system, has shown that the TiB_2 refiner particles only nucleate α-Al if coated with a thin layer of Al_3Ti. The α-Al was observed to nucleate on the boride basal faces with a well-defined orientation relationship with respect to both Al_3Ti and TiB_2. This is believed to be due to a good lattice match between the respective crystal structures. However, the Al-Y-Ni-Co alloy system, whilst having good glass forming capabilities, was somewhat removed from commercial Al alloy compositions used in industry. Research by Legresy [7] has revealed several Al-Ni-Si glass forming compositions that have a similarity to those used in industry, whilst retaining acceptable glass forming capabilities.

The aim of this study was to examine the effect of Si on heterogeneous nucleation in an $Al_{70}Ni_{13}Si_{17}$ alloy system using the metallic glass technique described above. The major emphasis was focused on the characterisation of the refiner rods and the nucleation of α-Al on TiB_2 grain refiner particles.

Experimental Methods

An $Al_{70}Ni_{13}Si_{17}$ master alloy was produced by arc melting pure Al (99.999 wt.%), Si (99.999 wt.%) and Ni (99.95 wt.%) in an inert He atmosphere. From this master alloy, a metallic glass was produced by free-flow chill-block melt spinning. 2-3 g of the master alloy was placed in a silica crucible and melt-spun in a He atmosphere. The melt was heated to a temperature of 900°C and ejected onto a Cu wheel rotating at a speed of 40 ms^{-1}. To ensure homogeneity, the charge was held for two minutes in the radio frequency induction field, which ensured continuous stirring before ejection. The resulting ribbons were approximately 3 mm wide and 30 μm thick. Ribbons were produced with and without grain refiner rod additions. In the former case, Ti-B-Al 5:1 grain refiner was added in the ratio of 0.16 g of rod to 10 g of the master alloy with the excess Al from the refiner rod subtracted from the master ingot before melt spinning. Both the Ti-B-Al rod and the melt-spun ribbons were examined using X-ray diffraction (XRD), TEM, and energy-dispersive X-ray spectroscopy (EDS). Thin foil specimens were made by electropolishing using a solution of 90% ethanol and 10% perchloric acid at a temperature of –30 to –40°C at 20 V. Specimens were placed in folded Cu grids before TEM examination was performed using Philips CM20 and JEM 3000 FEG microscopes operated at 200 and 300 kV respectively.

Results and Discussion

Microstructure of Refiner Rod

Figure 1 shows the microstructure of the Ti-B-Al grain refiner rod containing TiB_2 and Al_3Ti particles randomly distributed within the Al matrix. The Al_3Ti particles varied in size and morphology as a result of the thin foil sectioning. Arnberg et al. [8] have identified aluminide particles with three distinct morphologies; block, flake and petal. During casting, their shape and size was found to have a marked influence on the grain-refinement-contact-time as a result of differing dissolution times. However, no distinct shapes were found in the cold deformed refiner rod samples.

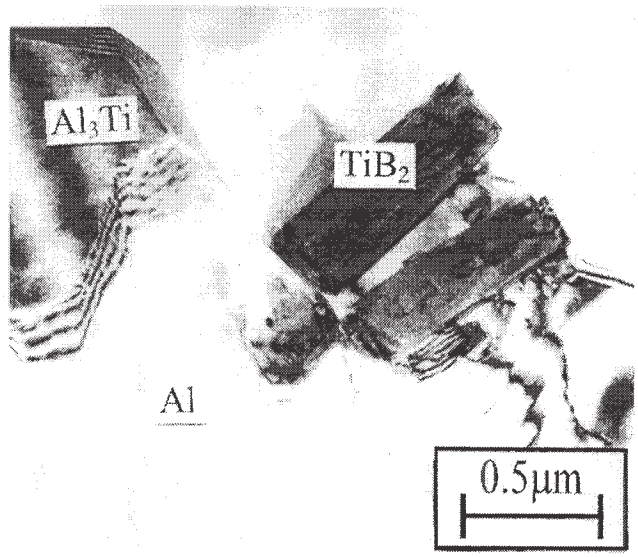

Figure 1. TEM micrograph of Ti-B-Al grain refiner rod, taken along the rod cross section, showing TiB_2 and Al_3Ti particles embedded within the Al matrix.

The boride particles exhibited a facetted, hexagonal platelet morphology with the {00.1} and {10.0} planes as their main faces. TEM examination of thin foils, prepared from the cross section of the rod, revealed that the particles were predominantly aligned so that their basal planes were close to an edge-on position, as illustrated in Figs. 1 and 2. This indicates systematic sectioning of the hexagonal platelets perpendicular to their {00.1} planes and, thus, their preferential orientation within the rod with these planes approximately parallel to the rod axis, as a result of cold deformation during the manufacturing process. Their diameter-to-thickness ratio was approximately 4:1 with the diameter of a majority of the particles being less than one micron. Corresponding diffraction patterns confirmed the TiB_2 hexagonal crystal structure with parameters a = 0.303 nm and c = 0.323 nm [8].

Selected-area diffraction (SAD) patterns obtained from the boride particles show two sets of perpendicular streaks parallel to [00.1] and [1$\bar{1}$.0] directions in reciprocal space (Fig. 2(d)). Thus, these streaks are indicative of a thin layer covering both their basal and non-basal faces. The presence of the layer was confirmed by dark field TEM imaging with the objective aperture placed on the streak between the centre and the (00.1) spot (Fig. 2(c)). The analysis of the SAD pattern in Fig. 2(d) revealed that the {00.1} and {111} planes corresponding to TiB_2 and Al respectively are approximately parallel. There was also an indication of possible weak spots located close to the {111} spots of Al that may correspond to {112} planes of Al_3Ti. This indicates the presence of an orientation relationship between the TiB_2, Al_3Ti layer and Al with the corresponding {00.1}, {112}, and {111} planes approximately parallel to each other. There is a strong similarity between these layers found in the grain refiner rod and those observed on TiB_2 particles within the Al-Y-Ni-Co glassy matrix by Schumacher and Greer [4,6] and identified as

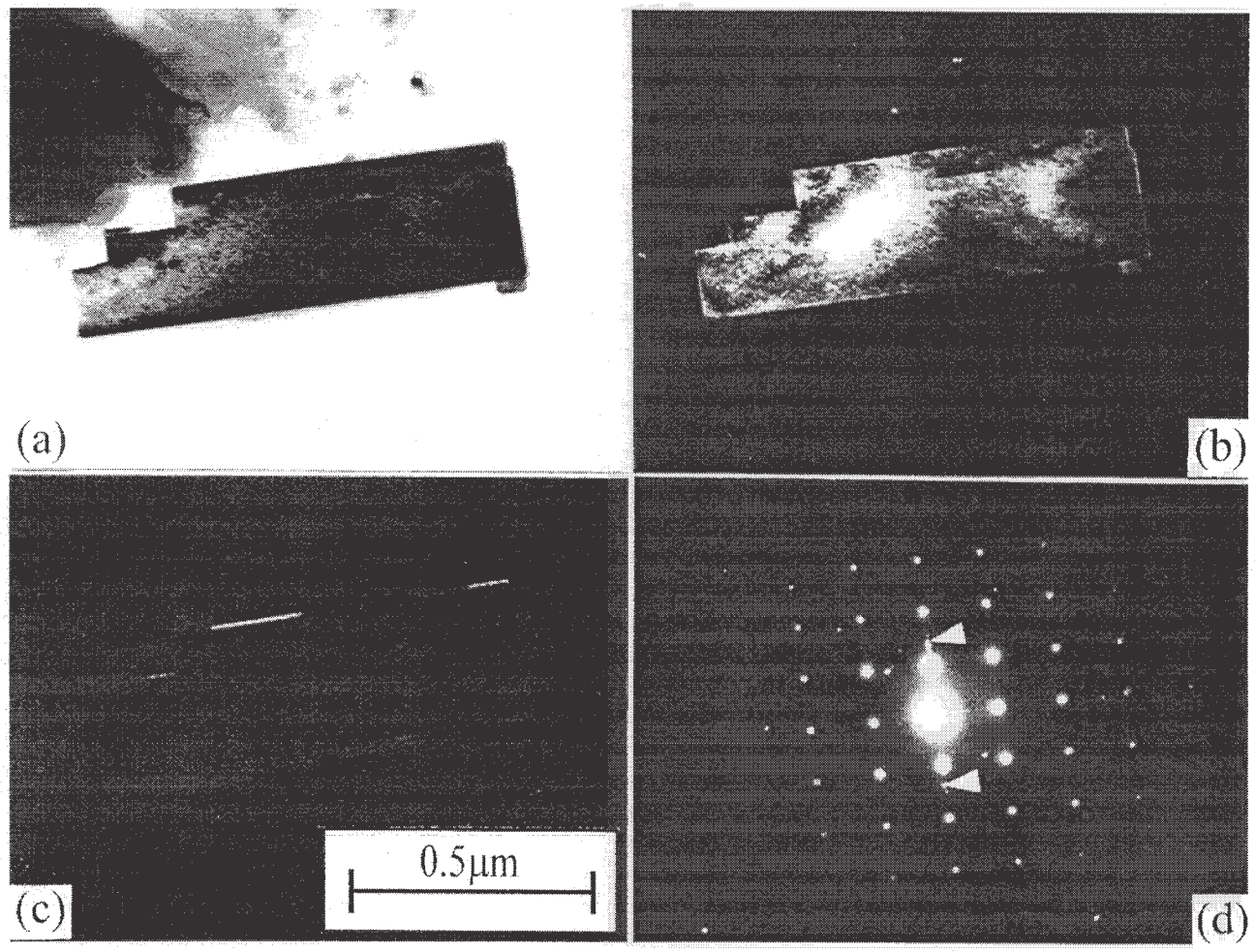

Figure 2. TiB_2 particle observed in the grain refiner rod coated with a thin layer: (a) TEM bright-field micrograph; (b) centered dark-field micrograph using {00.1} diffraction spot from the particle; (c) centered dark-field micrograph using the streak between the centre and {00.1} spots; (d) corresponding SAD pattern (zone axis [11.0]) with arrows indicating {111} Al spots.

Al_3Ti. In previous work, Schumacher and Greer [5] reported that the thickness of the aluminide layer was approximately 3 nm. The layer indicated in the dark-field micrograph in Fig. 2(c) is much greater than the above value. This can be attributed to specimen drift together with the long exposure time used.

The finding, indicating that layers are already present in the rod is significant in that it shows that the layer is not an artifact of the metallic glass technique. It also indicates that, in most instances, it is not formed in the melt although it can be enhanced or depleted. Thus, from the results obtained from the rod, it is suspected that the increased Si content, associated with Si poisoning, affects this aluminide layer, which subsequently has a detrimental effect on the borides ability to nucleate Al.

Melt-spun Ribbons

An XRD trace obtained from the Al-Ni-Si melt-spun ribbon, produced without the grain refiner rod addition, is shown in Fig. 3. The broad halo exhibited in this trace indicates that the ribbon was amorphous in character. This finding was further confirmed by the presence of diffuse rings in the SAD patterns, observed during TEM investigation of the above ribbon in Fig. 4. Both the XRD trace and SAD patterns acquired from the ribbon containing grain refiner particles were found to be similar to those shown in Fig. 3 and 4. This suggests that the matrix remained essentially unaffected by the presence of stable embedded TiB_2 particles.

No separate Al_3Ti particles, originally present in the grain refiner rod and known to serve as potent Al nucleation sites [8], were observed within the glassy matrix, which suggests that they completely dissolved in the melt. This was expected, as it was shown in the binary Al-Ti equilibrium phase diagram at the applied ejection temperature of 900 °C. It is necessary to note that, although the rod was added to the master alloy at addition levels greater than ten times that of commercial practice, the Ti content (0.05 wt.%) was still hypoperitectic, i.e. significantly lower than that required for the existence of stable aluminide within the melt, at the ejection temperature used.

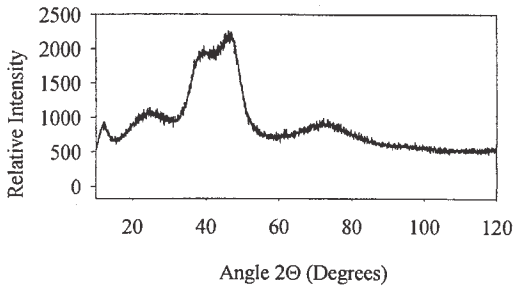

Figure 3. XRD spectrum obtained from the melt-spun ribbon produced without the grain refiner rod addition.

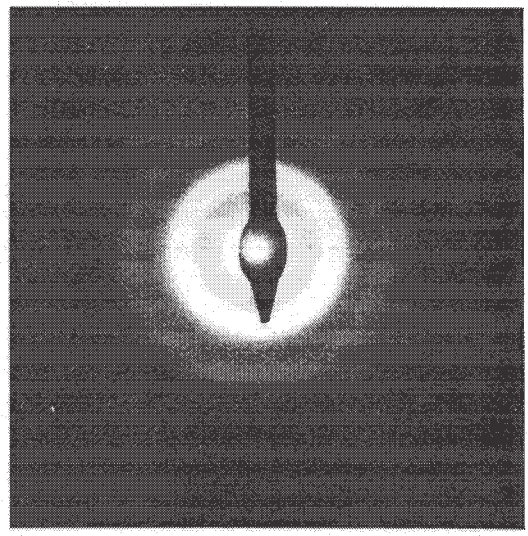

Figure 4. SAD pattern taken from the same ribbon as in Fig. 3.

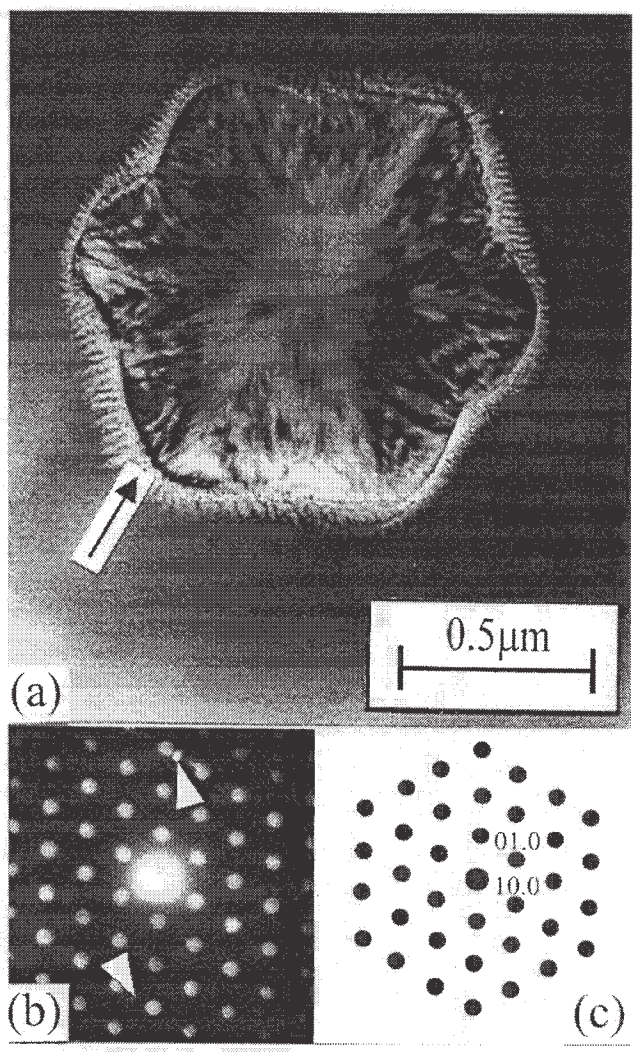

Figure 5. Hexagonal dendrite nucleating α-Al (arrowed) on its non-basal faces: (a) TEM bright-field micrograph; (b) micro-diffraction pattern from the interface between the dendrite and α-Al (arrows indicate {200} Al diffraction spots); (c) indexing of the pattern (zone axis [00.1]).

Within the glassy matrix, dendrites displaying a hexagonal shape were frequently observed (Fig. 5), having a hexagonal crystal structure with parameters (a = 0.664 nm, c = 0.377 nm) closely matching those found by Legresy [7] in the same alloy in the devitrified state. These dendrites nucleated copious amounts of Al without an apparent presence of a well-defined orientation relationship, as illustrated in the micro-diffraction pattern shown in Fig. 5(b).

Boride Particles

Boride particles found within the glassy matrix displayed no indication of α-Al nucleating on their basal or non-basal faces (Fig. 6). However, the borides were found to nucleate phases other than α-Al. This indicates that in casting practice, if pushed to solute-rich interdendritic regions, the boride particles could possibly nucleate intermetallics. Figure 7 shows an example of an unidentified phase nucleated on the non-basal faces of the TiB_2 particles and exhibiting a well-defined orientation relationship with these particles. EDS spectra acquired from this phase (Fig. 8) indicated the presence of Al, Ni, Si, Ti, S, Ar, Cu and Ca. The Cu and S were from the surrounding Cu grids, whilst it is probable that the Ar and Ca originated from impurities in the alloy or contamination during processing. EDS analysis of the boride particle, shown in Fig. 8(a), revealed that it consisted of a Ti-rich shell and an Al-rich core, as demonstrated by the spectra in Figs. 8(b) and 8(c). The observed presence of both TiB_2 and AlB_2 crystal structures, having very similar lattice parameters, within a single particle has been previously reported in [8] and is believed to be an artefact of the grain refiner rod manufacturing process [9].

Copious amounts of α-Al nuclei detected on the hexagonal dendrites indicate that the nucleation of Al was thermodynamically favorable under the present experimental conditions. However, its observed absence on the TiB_2 grain refiner particles contrasts with the results obtained in previous studies on the Al-Y-Ni-Co alloy system [4,6], where the borides were found to be coated with Al_3Ti layers with α-Al nucleating on their basal faces. The high nucleation potency of the boride

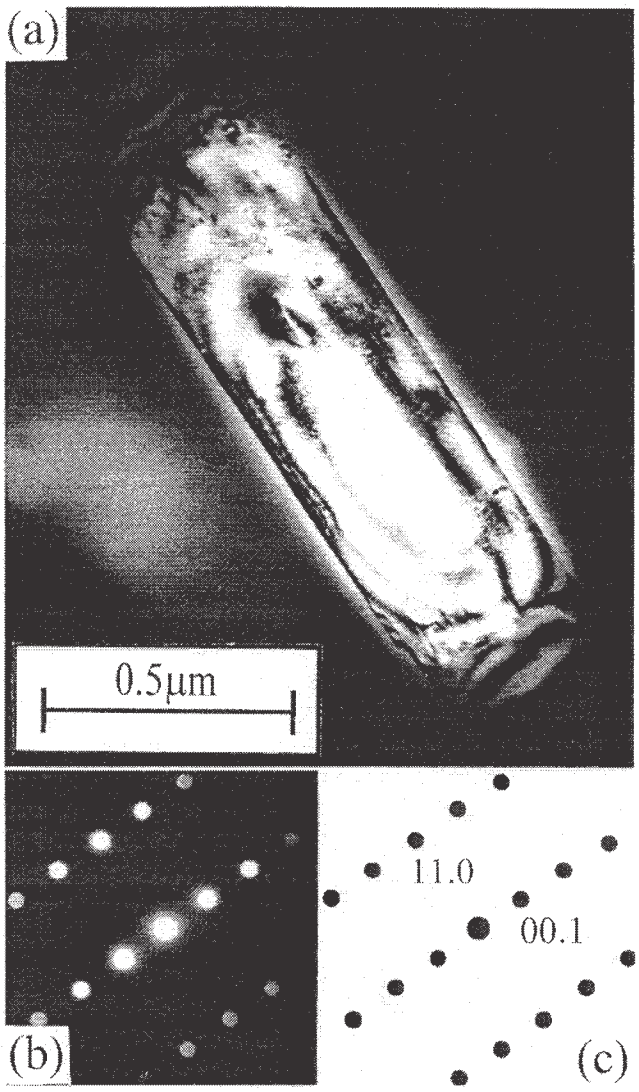

Figure 6. Boride particle showing no nucleation of α-Al: (a) TEM bright-field micrograph; (b) micro-diffraction pattern from the particle; (c) indexing of the pattern (zone axis [11.0]).

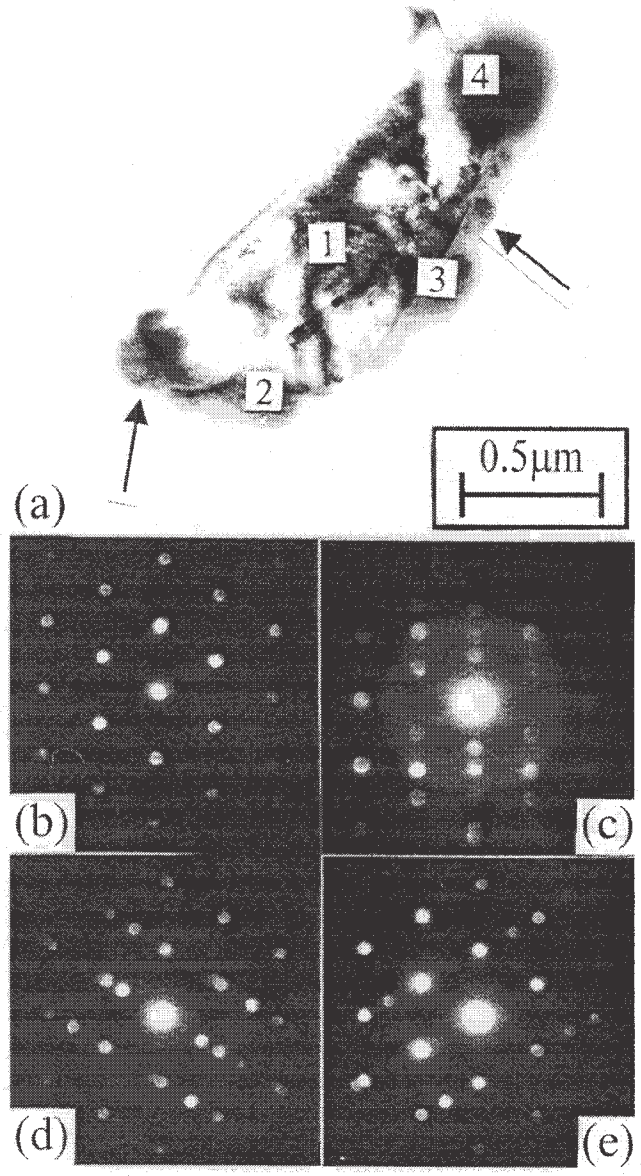

Figure 7. Boride particle with an unidentified intermetallic phase (arrowed) nucleating on its non-basal faces: (a) TEM bright-field micrograph (numbers indicate positions at which the micro-diffraction patterns were taken); (b) pattern from position 1 (zone axis [00.1] of the boride); (c), (d), (e), patterns from positions 2, 3, and 4 respectively, at the interfaces between the boride and the precipitating phase, showing three variants.

particles was attributed to the improved lattice match between the aluminide layer and the α-Al. The presence of these layers was determined in [4,6] by streaking in SAD patterns and dark-field imaging. On occasions, when thicker layers were observed, it was also possible to detect discrete diffraction spots corresponding to Al_3Ti [4,6]. In the present study, the observed streaks and the corresponding dark-field images indicate that the above layers are present on boride particles already in the grain refiner rod. However, SAD patterns taken from grain refiner particles within the glass only occasionally displayed faint streaks, which suggests that the layer is largely absent and, if locally present, is very thin and inconsistent. Thus, it appears that the Si within the melt was responsible for weakening the layer and the absence of α-Al nucleation. This supports the suggestion by Schumacher and Greer [4,5] that blank borides are poor nucleants of α-Al and the aluminide layer is necessary for the successful nucleation of α-Al. It is possible that a substitution of Si into the Al_3Ti layer beyond the solubility limit of $Al_3(Ti,Si)$ altered the corresponding lattice parameters and thus increased the crystal lattice misfit between the boride, aluminide layer and aluminium. This could explain both the observed desorption of the aluminide layers from the surface of the boride particles and the lack of α-Al nucleation on the weakened layers. Nevertheless, further detailed study is required to elucidate the effect of Si on the Al_3Ti layer.

The present results thus suggest that Si poisoning of the boride particles could be occurring, which is consistent with casting experience [1,2,3]. Previous studies [1,3] have attributed the Si poisoning effect to either the reduced nucleation potency of the

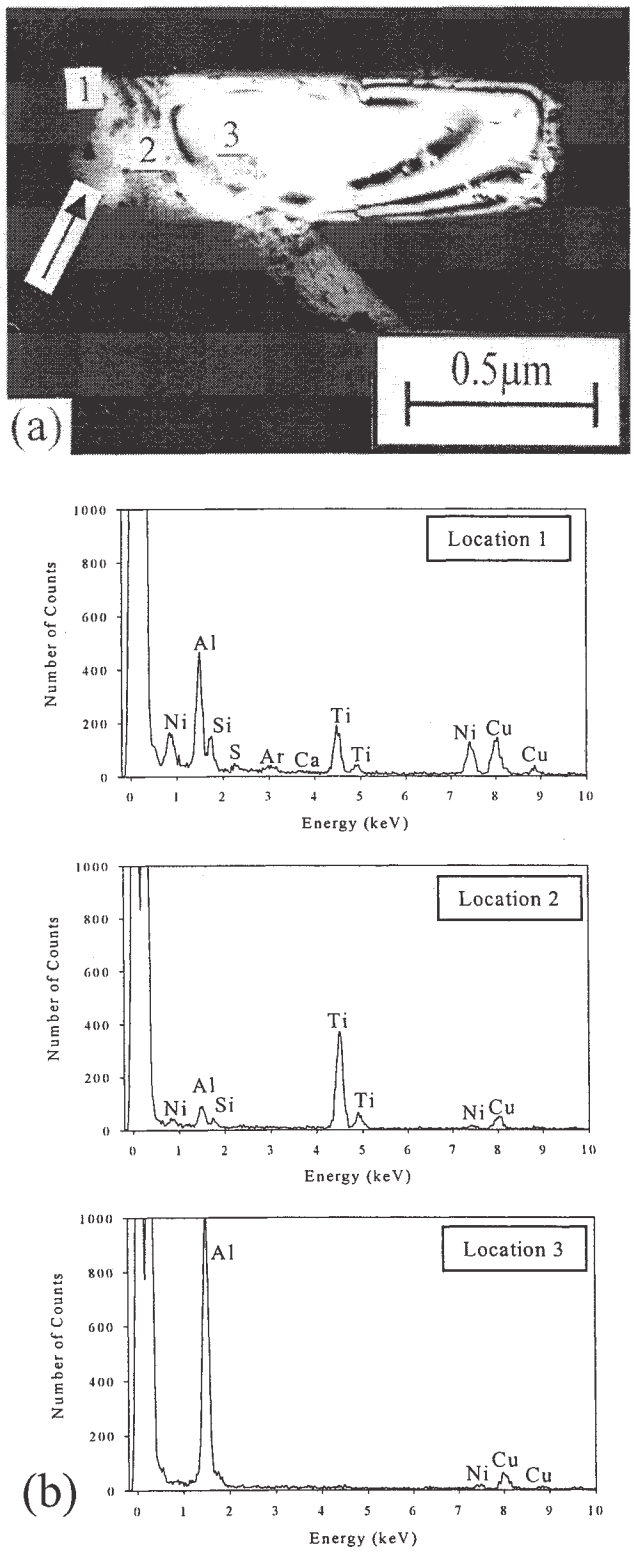

Figure 8. Cored boride particle nucleating an unidentified intermetallic phase (arrowed) analysed using TEM and EDS: (a) TEM bright-field micrograph (numbers denote locations from which EDS spectra were obtained); (b) corresponding EDS spectra.

boride particles or a reduction in growth restriction of the solid. The present results thus appear to indicate that the hindrance of α-Al nucleation is the dominant factor in the poisoning mechanism. This is also supported by Bunn et al. [10] who, although studying Zr poisoning, attributed this effect primarily to the nucleation stage of grain refinement, claiming that the reduction in growth restriction due to the presence of Zr was comparatively small.

Conclusions

Heterogeneous nucleation of α-Al in an $Al_{70}Ni_{13}Si_{17}$ alloy was investigated using a metallic glass technique. No nucleation of α-Al was found on TiB_2 grain refiner particles although it was frequently observed to occur on hexagonal dendrites during rapid quenching of the melt, which suggests Si poisoning of the boride particles. The observed presence of Al_3Ti layers on TiB_2 particles in the Ti-B-Al 5:1 grain refiner rod indicates that these layers can be formed during its production or on favorable holding conditions prior to solidification. It is known that these layers are necessary for the successful nucleation of α-Al. It appears that the increased Si content was responsible for the desorption of the aluminide layers from the surface of the boride particles, thus reducing their potency to nucleate α-Al.

Acknowledgements

Brian McKay (EPSRC-CASE studentship 97301785), Pavel Cizek (EPSRC GR/M12988), and Peter Schumacher (EPRSC Advanced Fellowship AF/97/25440) gratefully acknowledge financial support from the EPSRC in conjunction with London & Scandinavian Metallurgical Co. Ltd., Rotherham and Alcan International Ltd., Banbury. The authors would also like to thank Dr. Rafal Dunin-Borkowski for assistance with the operation of the JEM 3000 FEG microscope.

References

[1] J.A. Spittal, J.M. Keeble and M. Al Meshhedani, in J. Beech and H. Jones (eds.), *Proc. 4th Decennial Int. Conf. on Solidification Processing*, University of Sheffield, UK, 1997, p. 273.

[2] M.E. Birch and P. Fisher, in T. Sheppard (ed.), *Proc. Int. Conf. Aluminium Technology 1986*, The Institute of Metals, London, 1986, p117.

[3] M. Johnsson, *Z. Metallkd.*, *85* (1994) 781.

[4] P. Schumacher and A.L. Greer, *Mater. Sci. Technol.*, *14* (1998) 394.

[5] P. Schumacher and A.L. Greer, in W. Hale (ed.), *Proc. Int. Conf. Light Metals 1996*, TMS, Warrendale, PA, 1996, p.745.

[6] P. Schumacher, *PhD. Thesis*, University of Cambridge, 1990.

[7] J.M. Legresy, *PhD. Thesis*, l'Institut National Polytechnique de Grenoble, 1987.

[8] L. Arnberg, L Bäckerud and H. Klang, *Metals Technol.*, *9* (1982) 1,7.

[9] U.K Stoltz, F. Sommer, and B. Predel: *Aluminium*, *71* (1995) 350.

[10] A.M. Bunn, P. Schumacher, K.A. Kearns, C.B. Boothroyd and A.L. Greer, *Mater. Sci. Technol.*, *15* (1999) 1115.